Molecular BioSystems

Cite this: *Mol. BioSyst.*, 2011, **7**, 871–877

www.rsc.org/molecularbiosystems

PAPER

Alteration of microRNA expression correlates to fatty acid-mediated insulin resistance in mouse myoblasts†

Zhen-Ya Li, Hui-Min Na, Gong Peng, Jing Pu and Pingsheng Liu*

Received 11th October 2010, Accepted 18th November 2010
DOI: 10.1039/c0mb00230e

As new regulators at the post-transcriptional level, microRNAs (miRNAs) are non-coding 19–22 nucleotide RNA molecules that are believed to regulate the expression of thousands of genes. Since the monounsaturated fatty acid oleate can reverse insulin resistance induced by the saturated fatty acid palmitate, we carried out microarray analysis to determine differences in miRNA expression profiles in mouse muscle C2C12 cells that were treated with palmitate and palmitate plus oleate. Among the altered miRNAs, the expression levels of miR-7a, miR-194, miR-337-3p, miR-361, miR-466i, miR-706 and miR-711 were up- or down-regulated by palmitate, but restored to their original level by oleate. These results were verified by quantitative RT-PCR (QRT-PCR). Further studies showed that over-expression of miR-7 down-regulated insulin receptor substrate 1 (IRS1) expression as well as inhibited insulin-stimulated Akt phosphorylation and glucose uptake. The miRNA expression profiles correlated to oleate protection against palmitate-induced insulin resistance in mouse muscle cells offer an alternative understanding of the molecular mechanism of insulin resistance.

Introduction

Insulin resistance is one of the key factors responsible for type 2 diabetes mellitus and is associated with a significantly increased risk of concurrent abnormalities including obesity, hypertension, and cardiovascular disease.[1] Skeletal muscle accounts for most insulin-stimulated glucose utilization and is, therefore, the main site of insulin resistance.[2] Impairment of glucose utilization and insulin sensitivity has been related to the presence of high amounts of free fatty acids (FFA) in the plasma.[3] To mimic insulin resistant states in skeletal muscle, murine C2C12 myoblasts pretreated with saturated fatty acids often serve as a cellular model.[4] Interestingly, saturated and mono-unsaturated fatty acids differ significantly in their contribution to insulin resistance.[4,5] Previous studies have shown that oleate can reverse palmitate-induced insulin resistance and inflammation in skeletal muscle cells, however the intrinsic molecular mechanisms have not been fully elucidated.[6]

Recently, our understanding of complex gene regulatory networks governing cell physiology has evolved rapidly with the discovery of microRNAs (miRNAs). miRNAs are an abundant class of short endogenous non-coding RNAs that are about 19–22 nucleotides (nt) in length.[7] They negatively regulate the expression of many protein-coding genes through pairing interactions with the 3′ untranslated region (UTR) of their mRNAs, resulting in direct cleavage or translational repression in a combinatorial fashion.[8] miRNAs execute their functions in different cellular processes by targeting an estimated 10%–30% of all protein-coding genes.[9,10] Important roles for miRNAs have emerged in the control of metabolic pathways, as suggested by studies implicating miRNAs in the regulation of fat metabolism, adipocyte differentiation, energy homeostasis, glucose-stimulated insulin secretion, and insulin resistance.[11–14] In particular, recent studies that identified the miRNA signature related to insulin sensitivity in skeletal muscle reveal the involvement of miRNAs in post-transcriptional regulation of insulin resistance in this tissue.[15–17] Palmitate-altered miRNA expressions are also reported to contribute to fatty acid-mediated pancreatic β-cell dysfunction.[18]

In order to unravel the potential roles of miRNAs in the post-transcriptional events involved in insulin resistance and to comprehensively understand the complicated molecular mechanisms of insulin resistance from a new angle, especially the protective effects of oleate on palmitate-induced insulin resistance in skeletal muscle cells that consume about 70% blood glucose,[19] we used an insulin resistant C2C12 model that was identified to be instrumental in the study of insulin resistance.[20] We performed a microarray analysis which revealed distinct miRNA expression profiles in palmitate-treated, palmitate plus oleate-treated and normal C2C12 cells. The results of the microarray study were confirmed by quantitative RT-PCR (QRT-PCR). Using our microarray

National Laboratory of Biomacromolecules, Institute of Biophysics, Chinese Academy of Sciences, Beijing, 100101, China. E-mail: pliu@ibp.ac.cn; Fax: (8610) 65108517; Tel: (8610) 64888517

† Electronic supplementary information (ESI) available. See DOI: 10.1039/c0mb00230e

analysis data, we classified the altered miRNAs according to patterns in the changes of their expression level and analyzed them according to the GO function of their potential target genes. We found that several miRNAs, including miR-7, were up- and down-regulated by palmitate, but restored by palmitate plus oleate. Further studies on miR-7 showed that miR-7 acts as a mediator for palmitate-reduced insulin sensitivity and insulin receptor substrate 1 (IRS1) is one of the miR-7 target genes.

Materials and methods

Cell culture

Mouse myoblast cell line C2C12 (ATCC) and rat myoblast cell line L6 over-expressed with myc-Tagged glut 4 (L6-GLUT4myc, from Dr. Amira Klip, Division of Cell Biology, The Hospital for Sick Children, Toronto, Ontario, Canada) were cultured in Dulbecco's modified Eagle's medium (DMEM) and modified Eagle's medium (α-MEM) respectively, supplemented with 2 mM L-glutamine and 10% heat-inactivated fetal bovine serum (FBS) in humidified incubators at 37 °C and 5% CO_2. To set up the insulin-resistant cellular model, C2C12 cells were treated with freshly prepared DMEM containing 500 μM palmitate and FBS for at least 12 h before further investigation. To study the protective effect of oleate on palmitate-induced insulin resistance, C2C12 cells were simultaneously treated with freshly prepared culture medium containing 500 μM palmitate and 200 μM oleate for 12 h before further investigation. To detect insulin sensitivity C2C12 cells were transferred to a serum-free medium in the presence or absence of insulin.

RNA preparation

Total RNA from palmitate-treated, palmitate plus oleate-treated, and normal mouse C2C12 cells was prepared using the Trizol extraction technique. All RNA samples were treated with DNase I (Qiagen) according to the manufacturer's protocol. The quality and quantity of the RNAs was assessed by taking A_{260}/A_{280} nm readings using a NanoDrop1000 spectrophotometer (NanoDrop Technologies). RNA integrity was determined by running an aliquot of the RNA samples on a denaturing agarose gel, followed by staining with ethidium bromide. The ratio of 28S rRNA to 18S rRNA was 2 : 1, indicating that there was no detectable degradation in the RNA samples.

Microarray experiments

After quantifying the RNA on a NanoDrop instrument, samples were labeled using a miRCURY™ Hy3™/Hy5™ Power labeling kit and hybridized onto a miRCURY™ LNA Array (v.11.0, Exiqon). Scanning was performed with an Axon GenePix 4000B microarray scanner. GenePix pro V6.0 was used to read the raw intensity of the image.

The intensity of the green signal was calculated after background subtraction and the median value of four replicated spots of each probe on the same slide was calculated. The "Normalized Data" were obtained with U6-snRNA intensity as an internal control, Normalized Data = (Foreground − Background)/"U6-snRNA-2". Unsupervised hierarchical clustering and correlation analysis were performed on our miRNA expression profiles. Low intensity differentially expressed miRNAs (which had Foreground − Background intensities of <50 in two compared samples) were filtered before further screening. The threshold value used to screen up- and down-regulated miRNAs was a fold change >1.50 and a fold change <0.67. Based on the results from miRNA GO function analysis and target prediction, miRNAs of interest were further verified using QRT-PCR.

Conventional real-time RT-PCR and real-time assay of miRNAs

Conventional reverse transcriptase reactions were performed with a Takara reverse transcriptase reaction kit according to the user manual (Takara). The cDNA was then used as a template for real time-PCR quantification of the target genes using gene specific primers in combination with SYBR Real-time PCR master mix (Applied Biosystems). Differences in the levels of the target genes among the samples were converted into fold-changes using the $2^{-\Delta\Delta ct}$ method of Livak and Schmittgen.[21] Briefly, the relative level of the target gene normalized to beta-actin was calculated using the following equation: fold change = $2^{\text{Ct target (control)}-\text{Ct target (treatment)}}/2^{\text{Ct actin (control)}-\text{Ct actin (treatment)}}$.

miRNA reverse transcriptase reactions were performed with an ABI miRNA reverse transcriptase reaction kit (Applied Biosystems) according to the user manual. Briefly, a 7.5 μl reaction cocktail was prepared by mixing 5 μg of the RNA samples with an appropriate volume of DEPC H_2O, 50 nM stem–loop RT primer, RT buffer, 0.25 mM each of dNTPs, 3.33 U mL^{-1} MultiScribe reverse transcriptase and 0.25 U mL^{-1} RNase inhibitor. The cocktail was incubated for 30 min at 16 °C, 30 min at 42 °C, and 5 min at 85 °C. The cDNA was then used as a template for real-time PCR quantification of miRNAs using miRNA specific primers and TaqMan probes using TaqMan miRNA expression assays kit (Applied Biosystems). Real-time PCR was performed on an Applied Biosystems StepOne™ Real-Time PCR System according to the manufacturer's protocol using aliquots of cDNA equivalent to 25 ng of the total RNA in a total PCR reaction mixture of 50 μL [initial activation at 95 °C for 10 min followed by three-step cycling (45 cycles) of denaturation at 94 °C for 15 s, annealing at 55 °C for 30 s and extension at 72 °C for 30 s]. All reactions were performed in triplicate. Differences in the levels of miRNAs amongst the samples were converted into fold-changes using the $2^{-\Delta\Delta ct}$ method as described above except that the internal control was U6 snRNA.

2-Deoxyglucose uptake

L6-GLUT4myc myoblasts were cultured to confluence, differentiated and treated with fatty acids. After the treatments indicated, L6 myotubes were washed 3 times with warm Kerbs–Ringer Hepes buffer (KRBH) (120 mM NaCl, 25 mM Hepes, 4.6 mM KCl, 1 mM $MgSO_4$, 1.2 mM KH_2PO_4 and 1.9 mM $CaCl_2$, pH 7.4). The cells were stimulated with 100 nM insulin or incubated with KRBH buffer for 10 min, and 0.5 μCi 2-DG mL^{-1} and 50 μM unlabelled 2-deoxyglucose were then added for another 5 min. After the incubation, the

cells were washed 3 times with ice-cold KRBH buffer and then lysed with 1% SDS for 5 min before quantifying the radioactivity using a scintillation counter (1450 MicroBeta TriLux Microplate Scintillation and Luminescence Counter, PerkinElmer) according to the manufacturer's protocol. Non-specific 2-DG uptake was determined by quantifying the radioactivity of cells pretreated with 10 μM cytochalasin B for 10 min.

Prediction and experimental validation of miRNA targets

We sought to identify miR-7 target genes by bioinformatics prediction and experimental validation. The databases used for target prediction were microCosm (http://www.ebi.ac.uk/enright-srv/microcosm/htdocs/targets/v5/) and microrna.org (http://www.microrna.org/microrna/home.do). The sensor vector of each target gene was constructed by replacing the 3′-UTR of firefly luciferase with the 3′ UTR of the target gene in a pGL3cM vector (kindly provided by Professor Deepak Srivastava, University of Texas Southwestern Medical Center and Children's Medical Center, Dallas, USA). The primers for amplifying the 3′-UTRs of the target genes are shown in Table S1.† Reporter vectors containing miR-7 binding site sequences (~51 bp) were generated and used as positive controls. Synthetic miRNA mimic and negative control oligonucleotides were co-transfected with sensor vectors and the pRL-TK vector (as an internal normalization control) into HEK-293 cells and then incubated for 24 h. Luciferase activity was determined using a Dual Luciferase Reporter Assay System (Promega) and a TD20/20 Luminometer (Turner BioSystems). Each experiment was repeated three times, and means were used in comparisons.

Pre-miR duplex and miRNA inhibitor nucleofection

Synthetic pre-miR duplex, miRNA inhibitor and corresponding negative control oligos were delivered separately into C2C12 or L6 cells using an Amaxa® Nucleofector® according to the manufacturer's instructions. Briefly, cell pellets obtained after 90 × g centrifugation at room temperature for 10 min were resuspended in 100 μL Nucleofector solution to a final concentration of 1×10^6–5×10^6 cells/100 μL. The 100 μL sample was then transferred into an Amaxa-certified cuvette and subjected to nuclofection using the appropriate Nucleofector program. After nucleofection, the sample was immediately transferred from the cuvette to a 60 mm plate containing 2 mL of pre-warmed medium. Cells were treated, or collected for further investigation after culturing for 24 h.

Western blotting

Cells were lysed directly with 2X SDS sample buffer after the treatments indicated, sonicated twice (for 9 s each time, at 200 Watts), and denatured at 95 °C for 5 min. The samples were loaded onto a 10% Tris-glycine gel (Bio-Rad) and run for 120 min at 110 V. The proteins were then transferred onto a PVDF membrane (Millipore) for 2 h at 200 mA. Subsequently, membranes were blocked in 5% Blotto non-fat dry milk in TBST buffer containing 1% Tween-20 for 1 h and were probed overnight with the following primary antibodies: anti-IRS1 (1 : 5000, Santa Cruz), anti-actin (1 : 5000, Cell Signaling), anti-Akt (1 : 2000, Cell Signaling) and anti-phosphorylated Akt (1 : 2000, Cell Signaling). After incubating the membranes with a secondary antibody for 1 h, chemiluminescent immunodetection was employed. The signal was visualized by exposing the membranes to PerkinElmer ECL autoradiography film. Experiments were carried out at least twice using the same cell lysates.

Statistical analysis

All data are reported as the mean ± SEM. The statistical significance of alterations in the miRNA expression patterns among the three groups of C2C12 cells was determined using the Mann–Whitney un-paired two-tailed *t*-test. The statistical significance of alterations in the expression patterns of the miRNA targets was determined using the two-tailed Student's *t*-test. P values < 0.05 were considered statistically significant.

Results

Oleate reverses palmitate-induced insulin resistance in C2C12 cells

To establish an insulin resistant skeletal muscle cell model, C2C12 cells were incubated with high concentrations of a dietary saturated fatty acid, palmitic acid (PA), for 12 h and the effects of PA on insulin-stimulated Akt phosphorylation were examined as previously described.[6] As shown in Fig. 1, the insulin-stimulated p-Akt level was significantly reduced compared with the control after a 12 h incubation with PA. These data suggest that C2C12 cells cultured in excess PA developed insulin resistance. Meanwhile, treatment of C2C12 cells with a dietary mono-unsaturated fatty acid, oleic acid (OA), reversed PA-induced insulin resistance shown by the recovery of the p-Akt level (Fig. 1, lane 4 *vs.* 8). OA alone did not affect base- and insulin-induced Akt phosphorylation (Fig. 1, lane 1 *vs.* 5, lane 2 *vs.* 6). Thus, we used this cell model displaying oleate protection against palmitate-induced insulin resistance in muscle cells for further mechanistic study.

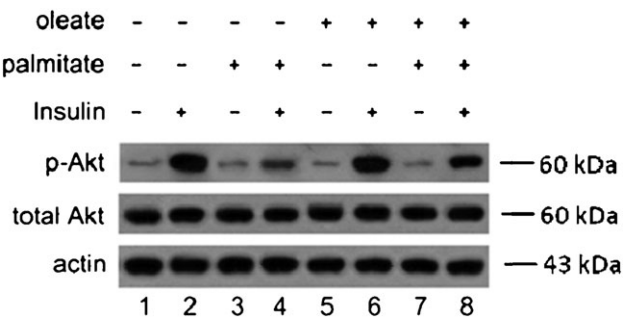

Fig. 1 Oleate reverses palmitate-induced insulin resistance in C2C12 cells. C2C12 cells were incubated for 12 h in the presence or absence of different fatty acids (0.5 mM palmitate, 0.2 mM oleate, or 0.5 mM palmitate plus 0.2 mM oleate). Cell lysates were assayed by Western blotting with antibodies against total and phosphorylated-Akt (Ser473).

Identification of miRNAs that are correlated with oleate protection against palmitate-induced insulin resistance

Using microarray techniques, we compared miRNA expression levels in C2C12 cells treated with palmitate alone or palmitate plus oleate. We screened and divided all altered miRNAs into four subgroups based on their expression patterns (Table S2†): (1) those up-regulated by palmitate compared with the control; (2) those down-regulated by palmitate compared with the control; (3) those up-regulated by palmitate plus oleate compared with palmitate alone; and (4) those down-regulated by palmitate plus oleate compared with palmitate alone. The pattern of seven miRNAs (6 miRNAs present in both groups 1 and 4; and 1 present in both groups 2 and 3) (Table 1) was correlated to the change in insulin signal caused by PA or PA plus OA. To validate the findings of the microarray studies, these miRNAs were first quantified by QRT-PCR. Trends in the changes in the miRNA levels were generally similar to those observed in the microarray studies (Fig. 2A). In particular, we detected the expression profiles of miR-7 over time in C2C12 cells treated by palmitate or palmitate plus oleate. Disparities in the miRNA expression profile curves between palmitate-treated C2C12 cells and palmitate plus oleate-treated C2C12 cells increased with treatment time (Fig. 2B), confirming that OA could block PA-induced miR-7 expression.

Negative effects of miR-7a on the insulin signaling pathway

As described above, several potential miRNAs were shown to be related to oleate protection against palmitate-induced insulin resistance in C2C12 cells. Based on GO function analysis of predicted miRNA target genes and the relative abundance of miRNAs, we chose miR-7a for further study. First, we examined the effect of miR-7a on the insulin signalling pathway by measuring the level of phosphorylated Akt. Pre-miR-7a duplex-nucleofected C2C12 cells which had undergone short-term exposure to insulin showed that Akt phosphorylation was significantly reduced compared with pre-miR-nucleofected controls (Fig. 3A). Since the mature sequence of miR-7 is highly conserved in mammals, we speculated that the function of miR-7 is also conserved and that pre-miR-7a duplex can be used to examine the effect of miR-7a on glucose uptake in rat muscle L6 cells. Results showed that miR-7a did indeed reduce insulin-mediated glucose uptake in L6 cells (Fig. 3B). Taken together, our results indicate that miR-7a has an inhibitory effect on the insulin signalling pathway, which partially resembles palmitate treatment-induced insulin resistance.

Table 1 Alteration of miRNAs correlates with oleate protection against palmitate-induced insulin resistance in C2C12 cells

	Fold Change (normalized data)	
Name	PA/con	(PA + OA)/PA
mmu-miR-7a	1.612	0.610
mmu-miR-194	1.571	0.429
mmu-miR-337-3p	1.815	0.345
mmu-miR-361	1.774	0.474
mmu-miR-466i	0.422	1.398
mmu-miR-706	2.040	0.417
mmu-miR-711	1.802	0.605

miR-7a inhibits IRS1 expression

Having shown that miR-7a plays a negative role in the regulation of the insulin signalling pathway, we analyzed and screened potential target genes by bioinformatic methods. Several putative miR-7a target genes (Table 2) were selected for further verification based on their function and the complementarity between miR-7 and the corresponding binding sites in the 3′-UTRs of their mRNAs. We cloned intact 3′-UTRs of each putative target gene mRNA using luciferase as a sensor to measure the effect of miR-7a. Sensor constructs were individually nucleofected with pre-miR-7 duplex or negative control pre-miR and the relative fold change of each construct was normalized to the internal control (Fig. S3†). In parallel, we tested the efficiency of our pre-miR-7a duplex transfection with a miR-7 positive control reporter construct, a plasmid containing two tandem, fully complementary, miR-7 target sites in the 3′-UTR of luciferase. Pre-miR-7 duplex dramatically down-regulated reporter gene activity, indicating high transfection efficiency and efficacy ($P < 0.001$; Fig. 4A). Of the putative target genes, the level of IRS1 mRNA and protein in pre-miR-7a duplex nucleofected C2C12 cells was further investigated by real-time PCR and immunoblotting. Consistent with results from the reporter gene assay, the IRS1 protein level was markedly decreased by pre-miR-7a duplex (Fig. 4C) whereas the IRS1

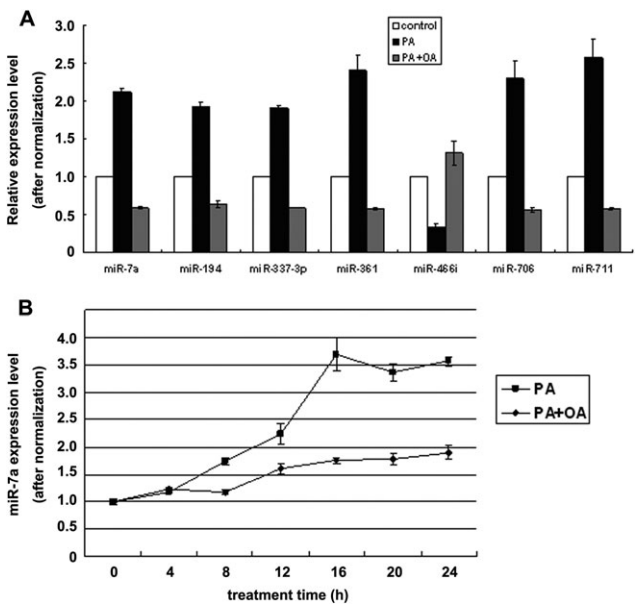

Fig. 2 Verification of miRNAs of interest using quantitative RT-PCR. (A) Expression levels of individual miRNAs in C2C12 cells treated with vehicle control, palmitate (PA) or palmitate plus oleate (PA + OA) were detected by QRT-PCR using miRNA-specific primers and normalized to the level of U6 snRNA expression. (B) Time course of miR-7a expression after exposure to palmitate (PA) or palmitate plus oleate (PA + OA). Changes in miRNA levels were determined by QRT-PCR and normalized against the expression level of U6. Values are presented as mean fold-change ± SEM ($n = 3$).

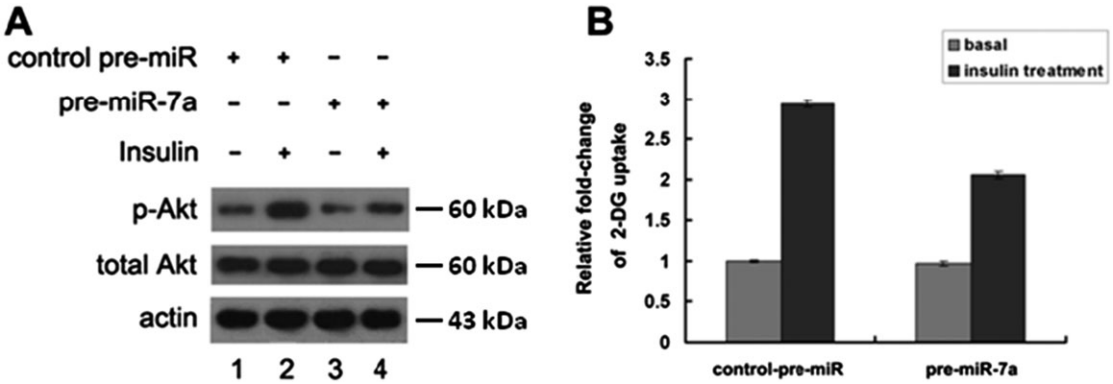

Fig. 3 miR-7a negatively regulates the insulin signalling pathway. (A) Levels of phosphorylated Akt (p-Akt) and total Akt in pre-miR-7a or control pre-miR nucleofected C2C12 after short-term insulin treatment, as detected by Western blotting. (B) [^{3}H]2-deoxyglucose uptake in pre-miR-7a or control pre-miR nucleofected L6 cells with or without insulin treatment was measured as described in the Materials and Methods.

mRNA level showed a decreasing trend, but not a significant change (Fig. 4B).

Discussion

As new members of the gene expression regulatory network, individual miRNAs are believed to moderately affect the expression levels of hundreds of target genes simultaneously.[22,23] In addition, a given target gene can be regulated by several functionally related miRNAs.[8] miRNA expression profile changes in response to a specific stimulus can provide useful information about the regulation of gene expression particularly at the post-transcriptional level. The miRNA array system is a high-throughput method for providing abundant information on miRNA expression profiles and will help us uncover post-transcriptional events related to insulin resistance. In this study, we identified several miRNAs related to oleate protection against palmitate-induced insulin resistance in skeletal muscle cells and thus provide a new approach for better understanding the complicated molecular mechanisms of insulin resistance.

Insulin signalling is mediated by a highly complex network controlling a variety of different processes. Briefly, in the presence of insulin, the insulin receptor phosphorylates the insulin receptor substrate (IRS) proteins, which are linked to the activation of two main signalling pathways: the metabolic phosphatidylinositol 3 kinase (PI3K)/protein kinase B (PKB, also known as Akt) pathway, responsible for most of the metabolic actions of insulin, and the mitogen-activated protein kinase (MAPK) pathway.[24]

Interestingly, miR-7 has been shown to decrease viability and invasiveness of glioblastoma cells by inhibiting the Akt pathway through down-regulation of IRS1 and IRS2 (Kefas *et al*., 2008). In our study, we found that miR-7a could be up-regulated by palmitate and restored by oleate (Fig. 2). Similar to previous report (Kefas *et al*., 2008) and predictions (Table 2), miR-7a also showed its inhibitory effect on the insulin signaling pathway by targeting IRS1 in C2C12 cells (Fig. 3 and 4). In addition, miR-7a may also target many glucose and lipid metabolic genes, such as phosphoenol-pyruvate carboxykinase 1 (PCK1) stearoyl-CoA desaturase (SCD), peroxisome proliferator-activated receptor alpha (PPARα), and peroxisome proliferative activated receptor gamma co-activator 1 alpha (PGC-1α) (Fig. S3†). Previous studies have shown that different effects of saturated and unsaturated fatty acids are related to their ability to promote DAG accumulation, and that palmitate resulted in the down-regulation of PGC-1α and acyl-coenzymeA: diacyl-glycerolacyltransferase2 (DGAT2), the enzyme that controls the rate of triglyceride (TAG) synthesis from DAG. In contrast, co-incubation of palmitate-exposed cells with oleate reversed these changes.[6]

When we attempted to use a miR-7a inhibitor to reconcile palmitate-induced insulin resistance in skeletal muscle cells the

Table 2 Potential miR-7a target genes in humans

Putative target gene	miR-7 target sequence	Function
Insulin receptor substrate1 (IRS1)	5′-aaGAGGAAAUUAAAGUCUUCCa-3′	**Insulin signaling**
Insulin receptor substrate2 (IRS2)	5′-uuAAUGGCAAUGCAAAAGUCUUCCu-3′ 5′-uuAACUUAUCUUGCUCUGUCUUCCa-3′	**Insulin signaling**
Insulin degradation enzyme (IDE)	5′-ugGAUGCAUUCCUGA GUCUUCCa-3′	**Insulin signaling**
Phosphoenolpyruvate carboxykinase 1 (PCK1)	5′-ugGGCAAGAUGACCUACUAGUUUUCCu-3′	**Gluconeogenesis**
Inositol hexaphosphate kinase 1 (IP6K1)	5′-ugguCACAAAUUACAGUCUUCUc-3′	**Inositol metabolism**
Phospholipase D1 (PLD1)	5′-cuAGUGAAUACAGUUUGUCUUUCa-3′	**Lipid metabolism**
Stearoyl-CoA desaturase (delta-9-desaturase) (SCD)	5′-acuAUAAGGUGCCUCAGUUUUCCu-3′	**Lipid metabolism**
Acyl-CoA synthetase long-chain family member 4 (ACSL4)	5′-agAAGAAAAUGUCUGUCUUUCu-3′	**Lipid metabolism**
Epidermal growth factor receptor (EGFR)	5′-ggAGCACAAGCCACAAGTCTTCCA-3′	**Cell growth and proliferation**
Peroxisome proliferative activated receptor gamma coactivator 1 (PPARGC1)	5′-**ucAGAGAGGUUAUUUGUUUUCCc-3′**	**Fatty acid oxidation**

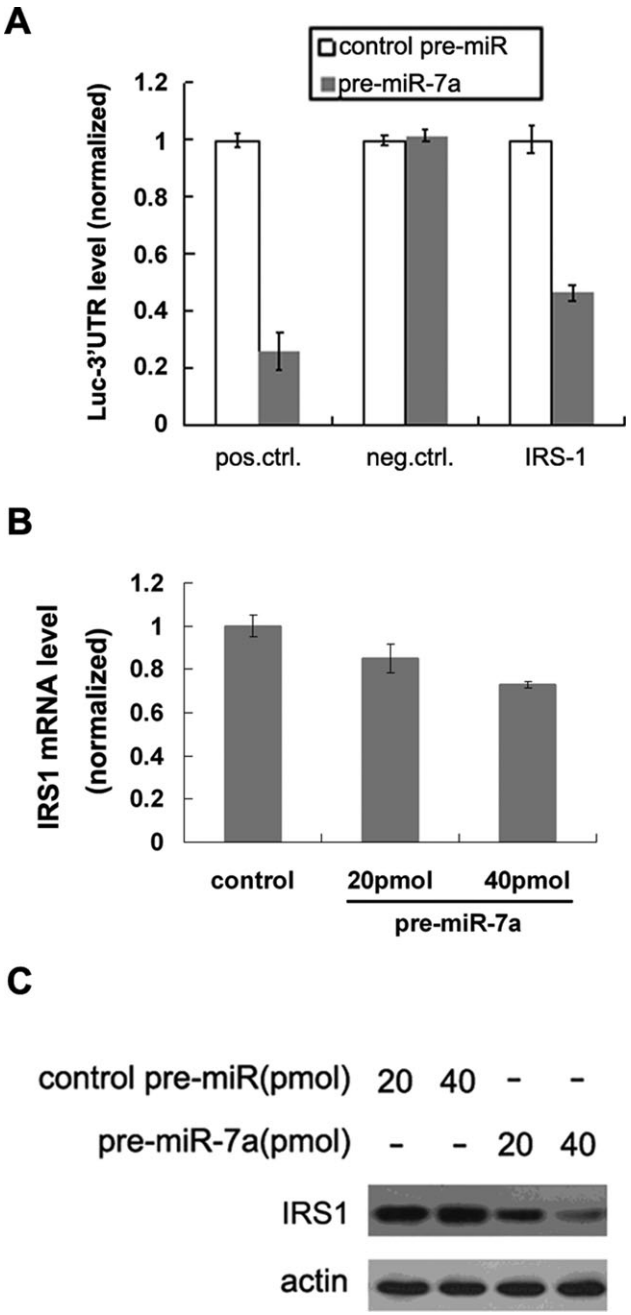

Fig. 4 miR-7a down-regulates IRS1 expression. (A) The expression of the IRS-1 3′-UTR reporter gene was inhibited when pre-miR-7a duplexes were cotransfected with a sensor vector containing the IRS-1 3′-UTR; (B) mRNA levels of IRS1 were reduced in skeletal muscle cells that were nucleofected with different concentrations of pre-miR-7a duplex or control pre-miR, incubated for 24 h. Results were analyzed by QRT-PCR, with actin mRNA levels used as an internal control. Data are presented as the mean ± S.D. of three experiments; (C) The protein level of IRS1 decreased in skeletal muscle cells that were nucleofected with different concentrations of pre-miR-7a duplex or control pre-miR, incubated for 24 h, and then analyzed by Western blotting using an anti-IRS1 antibody, with an actin antibody used as an internal control. In the Figure, pos. ctrl stands for positive control and neg. ctrl stands for negative control.

level of phosphorylated Akt did not recover markedly (data not shown). This may be due to one of two reasons. First, palmitate-induced insulin resistance is a very complicated process with many concurrent cellular events including the modification of insulin signalling molecules, inflammation, ER stress, and oxidative stress to mitochondria, and miRNA regulation may only be involved in some of these events. Second, the action of several miRNAs may be required for the regulation of a given cellular event. Our microarray results have shown that the expression levels of seven miRNAs were affected by palmitate and restored by oleate. miR-7a is therefore probably not the only miRNA that mediates palmitate-induced insulin resistance. Nonetheless, it is useful to use miR-7a to dissect molecular mechanism of insulin resistance and to develop a diagnostic marker. In addition, it is necessary to find other suitable miRNAs as intervention targets for the treatment of type 2 diabetes.

Abbreviations

miRNA, miR	microRNA
QRT-PCR	quantitative reverse transcriptase polymerase chain reaction
IRS1	insulin receptor substrate 1
3 UTR	3 untranslated region
PA	palmitic acid/palmitate
OA	oleic acid/oleate
FFA	free fatty acid
2-DG	2-deoxyglucose

Acknowledgements

The authors want to thank Drs Huina Zhang and Shunyan Zhang for their technical and administrative support. This work was supported by grants from the Ministry of Science and Technology of China (2006CB911001, 2009CB919000), and the National Natural Science Foundation of China (30871229, 30971431).

References

1 K. D. Bruce and M. A. Hanson, *J. Nutr.*, 2010, **140**, 648–652.
2 R. A. DeFronzo and D. Tripathy, *Diabetes Care*, 2009, **32**(Suppl 2), S157–163.
3 K. Cusi, *Curr. Diabetes Rep.*, 2009, **9**, 200–207.
4 C. Schmitz-Peiffer, D. L. Craig and T. J. Biden, *J. Biol. Chem.*, 1999, **274**, 24202–24210.
5 B. Vessby, M. Uusitupa, K. Hermansen, G. Riccardi, A. A. Rivellese, L. C. Tapsell, C. Nalsen, L. Berglund, A. Louheranta, B. M. Rasmussen, G. D. Calvert, A. Maffetone, E. Pedersen, I. B. Gustafsson and L. H. Storlien, *Diabetologia*, 2001, **44**, 312–319.
6 T. Coll, E. Eyre, R. Rodriguez-Calvo, X. Palomer, R. M. Sanchez, M. Merlos, J. C. Laguna and M. Vazquez-Carrera, *J. Biol. Chem.*, 2008, **283**, 11107–11116.
7 V. Ambros, *Cell*, 2001, **107**, 823–826.
8 D. P. Bartel, *Cell*, 2004, **116**, 281–297.
9 B. P. Lewis, C. B. Burge and D. P. Bartel, *Cell*, 2005, **120**, 15–20.
10 W. Filipowicz, S. N. Bhattacharyya and N. Sonenberg, *Nat. Rev. Genet.*, 2008, **9**, 102–114.
11 D. Iliopoulos, K. Drosatos, Y. Hiyama, I. J. Goldberg and V. I. Zannis, *J. Lipid Res.*, 2010, **51**, 1513–1523.
12 J. Krutzfeldt and M. Stoffel, *Cell Metab.*, 2006, **4**, 9–12.
13 S. Li, X. Chen, H. Zhang, X. Liang, Y. Xiang, C. Yu, K. Zen, Y. Li and C. Y. Zhang, *J. Lipid Res.*, 2009, **50**, 1756–1765.
14 A. A. Teleman, S. Maitra and S. M. Cohen, *Genes Dev.*, 2006, **20**, 417–422.
15 A. Granjon, M. P. Gustin, J. Rieusset, E. Lefai, E. Meugnier, I. Guller, C. Cerutti, C. Paultre, E. Disse, R. Rabasa-Lhoret,

M. Laville, H. Vidal and S. Rome, *Diabetes*, 2009, **58**, 2555–2564.
16 I. J. Gallagher, C. Scheele, P. Keller, A. R. Nielsen, J. Remenyi, C. P. Fischer, K. Roder, J. Babraj, C. Wahlestedt, G. Hutvagner, B. K. Pedersen and J. A. Timmons, *Genome Med.*, 2010, **2**, 9.
17 B. M. Herrera, H. E. Lockstone, J. M. Taylor, M. Ria, A. Barrett, S. Collins, P. Kaisaki, K. Argoud, C. Fernandez, M. E. Travers, J. P. Grew, J. C. Randall, A. L. Gloyn, D. Gauguier, M. I. McCarthy and C. M. Lindgren, *Diabetologia*, 2010, **53**, 1099–1109.
18 P. Lovis, E. Roggli, D. R. Laybutt, S. Gattesco, J. Y. Yang, C. Widmann, A. Abderrahmani and R. Regazzi, *Diabetes*, 2008, **57**, 2728–2736.
19 R. A. DeFronzo, R. Gunnarsson, O. Bjorkman, M. Olsson and J. Wahren, *J. Clin. Invest.*, 1985, **76**, 149–155.
20 V. Sarabia, T. Ramlal and A. Klip, *Biochem. Cell Biol.*, 1990, **68**, 536–542.
21 K. J. Livak and T. D. Schmittgen, *Methods*, 2001, **25**, 402–408.
22 X. J.-Z. Li Yong-Qing, Meng Zhi-Gang and Li Yong-Jin, *Acta. Biophys. Sinica*, 2007, **23**, 470–474.
23 L. P. Lim, N. C. Lau, P. Garrett-Engele, A. Grimson, J. M. Schelter, J. Castle, D. P. Bartel, P. S. Linsley and J. M. Johnson, *Nature*, 2005, **433**, 769–773.
24 A. R. Saltiel and C. R. Kahn, *Nature*, 2001, **414**, 799–806.